A Data Mining Approach to Validating Drillhole Logging Data in Pilbara Iron Ore Exploration

Daniel Wedge[1], Andrew Lewan[2], Mark Paine[2], Eun-Jung Holden[1] and Thomas Green[2]

[1]Centre for Exploration Targeting, The University of Western Australia, Crawley WA 6009, Australia
[2]Rio Tinto Iron Ore, 152-158 St Georges Terrace, Perth WA 6000, Australia

Abstract

Logging of exploration drillholes is a routine practice and its accuracy is essential for resource evaluation and planning in the minerals industry. Logged compositions record a set of material types with standardized mineralogy and texture characteristics. The material types logged may vary due to diversities in mineralization and geology, but also due to subjective biases and human error, leading to significant challenges for the industry. Thus, there is a need to validate the field logging whereby the material types and their percentages are adjusted to reconcile with laboratory assay values, while retaining the physical characteristics and geological context.

We introduce the Auto-Validation Assistant (AVA) algorithm that applies data mining methods to geologists' validation patterns recorded in a training process over hundreds of intervals of iron ore exploration drillholes. The AVA modifies the material types selected in the logged composition and their percentages according to geological rules learned in the training process, and proposes to the geologist a number of validated compositions with optimized geochemistry and mineralogical hardness, while also considering visible properties such as chip shape and color. Using the confidence value provided with each validated composition, the geologist can make informed validation decisions and remains in control of the validation process, while harnessing computational power.

Experiments were conducted to evaluate the auto-validated compositions generated by AVA: one to analyze the acceptance rate of the AVA generated compositions by geologists for 1,996 intervals in drillholes from different sites; and the other to compare manual and AVA-validated compositions using 14,600 drillholes from one entire deposit. The results showed the acceptance rate of AVA-validated compositions (without further change) of 74.3%, leading to significant time savings over tedious manual validation, while demonstrating that AVA provides comparable but more consistent results. The algorithm is fast and repeatable and can be adapted to different material types and training datasets, with potential applications beyond iron ore exploration.

Introduction

Rock samples from drillhole data provide mineralogical details crucial for orebody modeling and mining. A conventional mining exploration process involves drilling, logging and assaying exploration holes to better understand the structures and mineralogical compositions of an area (Sommerville et al., 2014). The modeled orebody volume, shape and grade form the basis of resource estimation block models for mining and planning purposes. However, drillhole logging is challenging due to the visual and textural ambiguity of some mineralogical types in small chip samples. Thus, the logging heavily relies on geologists' ability and subjective biases, which leads to variable outcomes.

Incorrect drillhole logging can result in outcomes with significant financial implications. In particular, in iron ore exploration and mining, ochreous goethite material and shale are commonly confused due to similarities in color and texture in chip samples obtained from reverse circulation (RC) drilling. However, these types are chemically very different, shale that is enriched in kaolinite is high in silica and alumina and low in iron, whereas ochreous goethite has a high iron grade but is much lower in silica and alumina than shale. Another property of ochreous goethite is its water holding capacity due to high levels of microporosity (Paine et al., 2016). As a result, it is sticky and causes problems such as blocking screen decks as shown in Figure 1, and ore transfer chutes, leading to unplanned downtime. Thus, there is a need to validate the logging data in order to improve the

robustness of resource estimates, and provide more accurate knowledge of the distribution of ochreous goethite which can assist in planning blending strategies to manage risks in mining.

Figure 1: Accurate modeling of ochreous goethite is necessary to prevent handling problems such as this blocked screen. From Paine et al. (2016).

Given that the logged composition summarizes the interval as percentages of material types, each type having average theoretical assay values, the interval's theoretical assays can be estimated from the logging. Validation involves adjusting the percentages of the logged material types, and adding or removing material types where necessary using geologically informed substitutions so that the theoretical assay values are within an error tolerance of the laboratory assay values obtained from the interval's chip samples. Error tolerances are used here not only as a measure of logging error, but also to allow for variability in the chemistry within each material type. To mitigate these variations, theoretical assays for each material type are maintained independently from site to site, and their values are routinely updated via reconciliation against plant data. Mineralized material types exhibit only small variations in Fe grade of up to 5%, though for most mineralized types the variation is less than 2%. Other material types may exhibit more variation though for product grade prediction, this is not a concern because waste material corresponding to these types is not typically processed through the plant.

In the following sections, we discuss logging and validation, the process of applying machine learning to recorded validation data, and deriving geologically feasible combinations of material types. Then we introduce the Auto-Validation Assistant (AVA) algorithm, which utilizes this training data and exploits computational power to explore a large space of possible solutions, of which a small number are proposed to the geologist. Finally we evaluate AVA on iron ore exploration projects in the Hamersley province in Western Australia.

Logging and Validation

RC drilling produces chip samples from which the logged compositions are estimated. Chip samples for each 2m interval are brought to the surface, and a rotary cone splitter used to divide the chips into equally distributed samples. Chips from one sample are logged by scooping a cup of material from the slurry, passing it through a sieve and estimating (1) the percentages of various material types present in the sieve (usually in increments of 5%), (2) the sample color, (3) the chips'

shape, and (4) the recovered percentage (Sommerville et al., 2014). The other sample is sent for laboratory XRF assay analysis, to measure Fe, SiO_2, Al_2O_3, P, S, Mn, MgO, TiO_2, CaO, Total LOI, LOI425 (typically indicating goethite-bound water) and LOI650 (typically indicating kaolinite associated water) measurements. Total Fe and Mn values are reported rather than their oxides due to their different possible oxidation levels. Additionally, using total Fe provides consistency with Fe units used elsewhere in resource estimation.

A logged composition for each 2m interval estimates the percentages of the interval's chips in terms of material types. The Material Type Classification Scheme (MTCS; Box et al., 2002) was developed to standardize primary characteristics, such as mineralogy and texture, in a hierarchical manner. It models physical and chemical attributes to predict metallurgical behavior and product quality for optimal ore processing (Paine et al., 2016). Each material type has theoretical assay, hardness, and lump-fine splits corresponding to particles larger or smaller than 6.3mm, with corresponding lump-fine geochemistry differences, thus enabling downstream estimation of a theoretical assay value, as well as lump-fine splits and handling characteristics of an orebody. Material types have been defined to be identifiable at scales ranging from microscopic (polished block) to macroscopic (chips, hand specimen and face scales). These qualitative physical properties remain consistent from site to site, though minor changes in geochemistry and physical properties such as lump % may occur. Some selected material types are listed in **Error! Reference source not found.**.

Goethite dominant mineralogy	
GOE	Earthy goethite
GOL	Ochreous goethite
GOV	Vitreous goethite
Hematite goethite mineralogy	
H2F	Microplaty hematite + martite (friable)
H2H	Microplaty hematite + martite (hard)
H2M	Microplaty hematite + martite (medium)
Hematite dominant mineralogy	
HGF	Martite-ochreous goethite + goethite
HGM	Martite ± microplaty hematite + goethite
HGH	Martite-vitreous goethite + goethite
Selected waste lithology codes	
SHL	Shale
SID	Siderite
BIF	Banded iron formation (waste)
CAL	Calcrete
CHT	Chert
CLA	Clay

Table 1: A subset of commonly-used codes from the MTCS

During validation, the logged composition is adjusted to match the assay values using geologically informed addition or removal of material types and adjusting their percentages, resulting in a validated composition. Validation cannot be performed in a vacuum; the original field logging provides an important source of information and must be used to inform the validation. In validation, there must be some common thread linking the interchanged material types. For example, two types may be swapped if they share similar physical characteristics, but significantly different chemistry. Some material types are physically distinctive and their presence is obvious, including pisolite. The percentages of these logged types may be altered within a logging error bound, but the type should never be removed or added. Thus validation is not just a goal-seeking exercise to minimize the assay error; a number of geological and physical constraints must also be satisfied. The validation process is summarized in Figure 2.

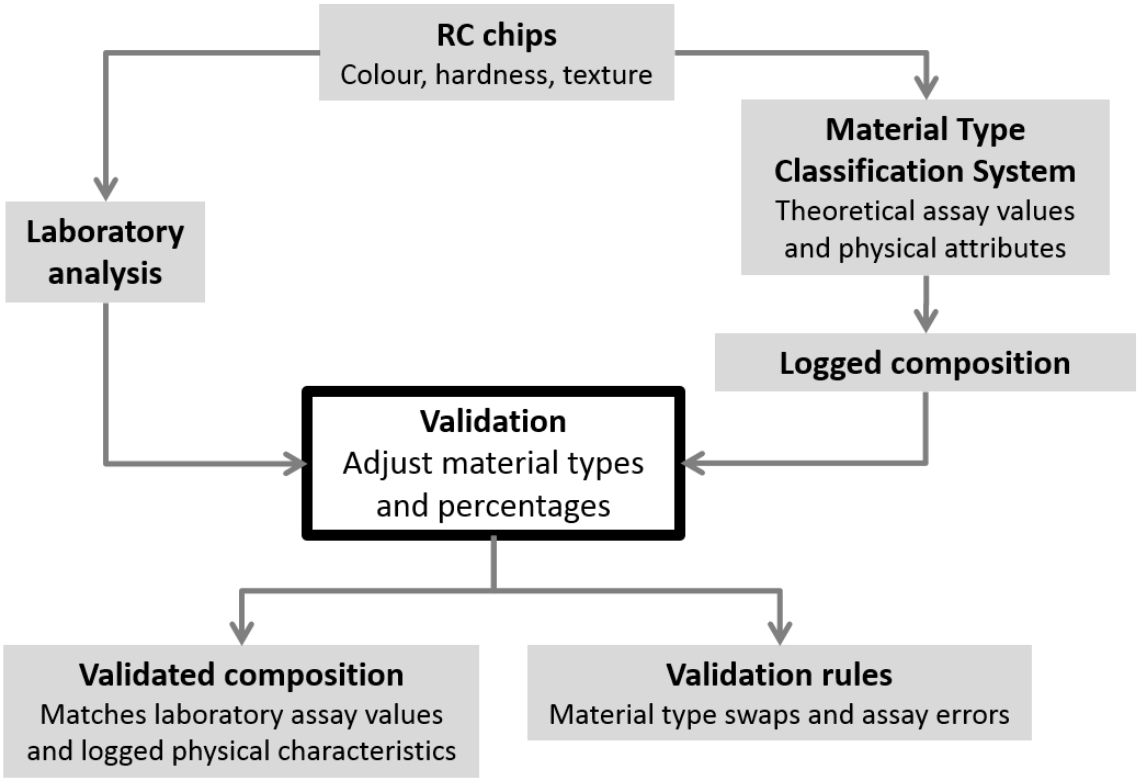

Figure 2: The relationships between validation and the logged and validated compositions.

Validation is time consuming, laborious and often inconsistent between geologists. On average, each 2m interval of an RC hole takes a number of minutes to validate. As hundreds of kilometers of RC holes are drilled each year by Rio Tinto Iron Ore in the Pilbara (Sommerville et al., 2014), it is therefore an extremely labor intensive task.

Data Mining of Validation Patterns

To understand geologists' validation patterns and provide training data for our algorithm, 11 experienced geologists were recorded performing validation. Data was collected through validation of 6 holes: 3 holes from one site and 3 from a second site, from iron ore deposits within the Marra Mamba formation and Brockman Iron Formation in the Hamersley Province. The Marra Mamba Formation is a banded iron formation (BIF) structure interleaved with shale bands (Trendall and Blockley, 1970). It is overlain by the Wittenoom Formation (Trendall and Blockley, 1970) which consists of dolomite, chert and shale. The Wittenoom Formation itself is overlain by the Mount Sylvia Formation, the Mount McRae Shale, and then the Brockman Iron Formation, which is another BIF structure interleaved with shale bands. The Brockman Iron Formation itself comprises the Dales Gorge Member, overlain by the Whaleback Shale, which itself is overlain by the Joffre Member (Trendall and Blockley, 1970). Hamersley Detrital deposits, located further up the stratigraphic sequence, are derived from weathered bedded ores (Morris, 1994).

Each hole was logged by a different field geologist. This provided different sources of error, reflecting geologists' varied training and biases. A further 20 standard intervals were validated, in which theoretical assays were computed from known material type combinations and provided alongside plausible but deliberately incorrect logging for the user to validate. The geologists validated 4,520 intervals in total.

Step-by-step changes from the logged to the validated compositions were recorded where for each step, validators swapped some percentage of one material type directly for another material type with similar physical characteristics, while reducing the total assay error. This allowed the incremental improvements to be captured, between the logged composition and the validated

composition for each interval. At each step, we recorded the difference between the theoretical assay value and the actual laboratory assay value (i.e. assay error), along with the material types swapped by the validator. The assay error is a 12-element vector, one component per element in the assay suite. Normalization was applied by dividing the vector by the maximum magnitude element so all elements have values between -1 and 1 (inclusive), then each element was rounded to the nearest 0.2, giving a normalized assay error. This produced a set of validation rules, where for a given normalized assay error, some percentage of one material type was removed and the same percentage of another material type added (which we term the material type swap).

We built a database of validation rules where each rule comprises the normalized assay error, the material type with increased percentage, the material type with reduced percentage, and the stratigraphic class containing the training interval. Each validation rule has a weight based on the percentage change in composition. Rules with identical keys were combined by summing the weights of the individual rules, thus repeated observations of a rule increase its weight. Rounding the normalized assay error vector increases the likelihood of rules being merged, reducing the size of the database. While this causes a minor inaccuracy in the calculation of the angle, described later, between the actual assay error vector of a composition and the normalized assay error, it is offset by reducing the number of very similar database rules through which to search, and the resulting states resulting from applying the same material type swaps with slightly different normalized assay errors would eventually be identified and merged by the algorithm.

We used three stratigraphic classes: detrital deposits, mineralized bedded, and shales. These respectively correspond to the: Hamersley detritals; mineralized Marra Mamba and mineralized Brockman; and BIF shale bands and Wittenoom Formation intervals in our training data. The rules are partitioned into different stratigraphic classes as some material type swaps will be confined to a specific class. For example, ochreous goethite is commonly swapped for clay in detritals, but is geologically unusual elsewhere as one would instead substitute ochreous goethite for shale. This partitioning also allows us to assign different weights to the same swap with the same assay error in different strata.

The material types swapped during training from one site are visualized in a chord diagram in Figure 3A. Swaps involving ochreous goethite (GOL) are highlighted for clarity in Figure 3B. The thickness of the chords joining two MTCS codes is proportional to the amount of material swapped (the swap direction is not shown). To reduce the complexity of the chord diagram, only material types with total material swapped above a threshold value of 2.2% of the total swapped volume are included, except for H2H and GOV, which are included to complete their mineralogical “families”.

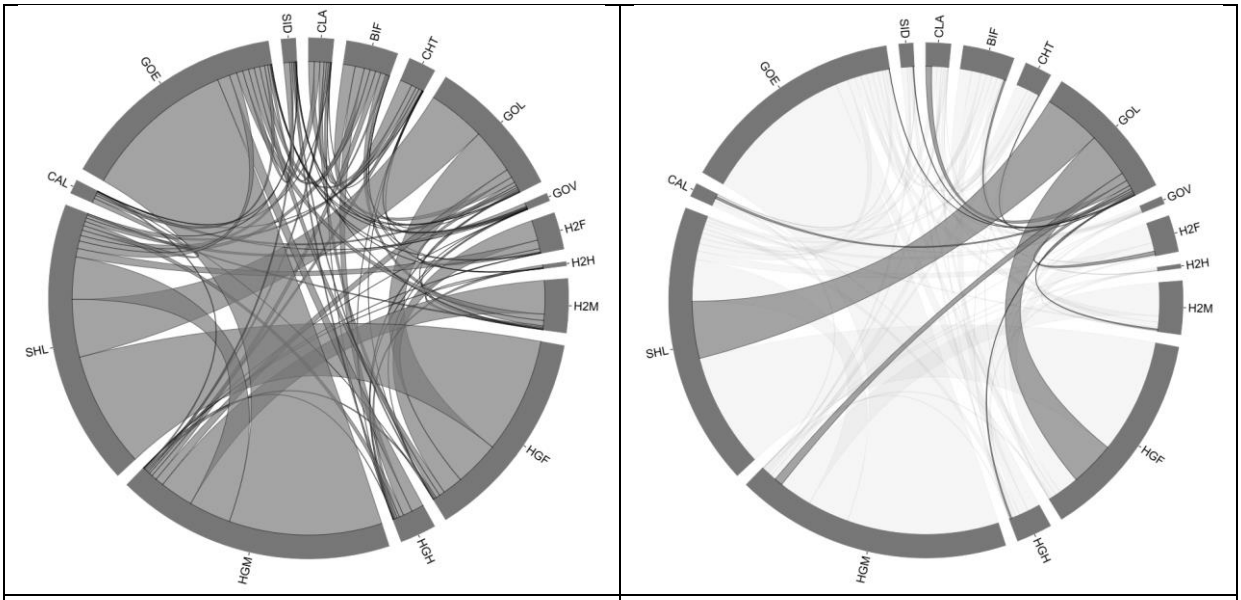

Figure 3: (A) Material type swaps observed in intervals from one site. (B) Highlighting the swaps involving ochreous goethite. Descriptions for the MTCS codes are given in Table 1.

The chord diagrams show that the dominant material type swaps are GOE-HGM, SHL-HGF, GOL-SHL, and GOL-HGF. These findings agree qualitatively with common knowledge, and allow the magnitudes of these changes to be quantified. For example, during the validation process, GOE may be removed for HGM (containing some hematite) if a higher theoretical Fe grade and lower LOI425 value is necessary to match the laboratory assay values. Physically, they are both of medium hardness and have lower lump characteristics, which is why GOE is preferentially interchanged with HGM instead of a harder type such as HGH. GOL and HGF are interchanged for similar reasons. SHL and GOL are easily confused in logging as they share similar physical characteristics, being soft and yellow, yet chemically they are very different: SHL represents kaolinite high in SiO_2, Al_2O_3 and LOI650 and low in Fe, whereas GOL is predominantly goethite with a moderately high Fe grade and has a high LOI425 value.

While the validation rules record which material types were swapped, we also learn which material types were commonly logged in conjunction with other types to understand the geological context of the material types. We adapted and extended a method known as the Apriori algorithm (Agrawal and Srikant, 1994) to determine association rules, whereby logging a set of, or individual, material types *X* leads to another material type *Y* being included in the same composition. Each association rule has confidence value, defined as the percentage of compositions containing *X* that also contain *Y*. The support for an association rule is defined as the percentage of compositions containing both *X* and *Y*.

The dataset that we used as input for the Apriori algorithm included over 60,000 intervals each with logged and validated compositions. This was far larger than the dataset used to form the database of the validation rules, since only the logged and validated compositions are required (i.e. not the individual swaps made during validation). We ran the Apriori algorithm independently for intervals from each of the three stratigraphic classes, since geological rules may vary according to stratigraphy. For example, kaolinite should be logged as the clay MTCS type in detritals, but as the shale type elsewhere. These patterns are implied in the outputs. We mined association rules with a minimum support value of 0.1% (per stratigraphy) and a minimum confidence value of 0.1% to identify only significant trends in compositions.

From these association rules, a set of material type compositions was generated where each composition was formed from the union of the material types in *X* and *Y*. This is for the purpose of

creating a list of subsets of geologically valid material types. **Error! Reference source not found.** shows the most common subsets of material types in each stratigraphic class.

Goethite dominant mineralogy	
GOE	Earthy goethite
GOL	Ochreous goethite
GOV	Vitreous goethite
Hematite goethite mineralogy	
H2F	Microplaty hematite + martite (friable)
H2H	Microplaty hematite + martite (hard)
H2M	Microplaty hematite + martite (medium)
Hematite dominant mineralogy	
HGF	Martite-ochreous goethite + goethite
HGM	Martite ± microplaty hematite + goethite
HGH	Martite-vitreous goethite + goethite
Selected waste lithology codes	
SHL	Shale
SID	Siderite
BIF	Banded iron formation (waste)
CAL	Calcrete
CHT	Chert
CLA	Clay

Table 2: Observed commonly co-logged subsets of material types

The common presence of clay in detrital intervals, high grade hematite and goethite types in mineralized bedded intervals, and shale in shale intervals is expected. While the data collected through these steps provides some insights into the validation process and geological context of material types, it more importantly forms the training data for our algorithm.

Auto-Validation Assistant (AVA)

The AVA algorithm mimics the human validation process while exploiting computational power. It applies material type swaps from the training data collection phase and geological rules mined by the Apriori algorithm to produce geologically plausible validated compositions with theoretical assay values closely matching the laboratory assay values. The algorithm's outputs are auditable, and training rules can be updated easily without requiring reprocessing all of the training data. A set of proposed validated compositions are presented, from which users can select what they judge as the best result. A geologist can also modify the proposed result by adding or removing material types, and modifying the percentages. Thus, geologists' knowledge and experience still play a crucial role in validation. The algorithm's name implies that it assists the user, while the geologist is still in control of the final validated composition, rather than being fully automated.

A geologist iteratively applies material type swaps to the logged composition to produce a validated composition. Although there is no limit to the number of swaps, a median of three swaps was observed. The AVA algorithm is a parallel version of this framework and the overview is shown in Figure 4. A swap selection process determines how to apply the training data to the logged composition. Swaps are applied in parallel and produce numerous parallel intermediate states in each iteration. An optimization is applied to each intermediate state to select the percentages for each selected material type to minimize a cost quantifying the differences in the assay and hardness values. These steps are described in detail below. The cost is used to rank the intermediate states. The best-ranked intermediate states are selected and the process repeated beginning with the intermediate states in place of the logged composition. A tree of compositions is therefore created, stemming from the logged composition. We used 40 intermediate states, and five iterations. These values were selected empirically as a trade-off between accuracy and time; these parameters acceptable results within five seconds, and 96% of manual validations during training required five or fewer material type swaps. A

final selection of states is then made by incorporating further geological criteria, and these proposed validations are presented to the user.

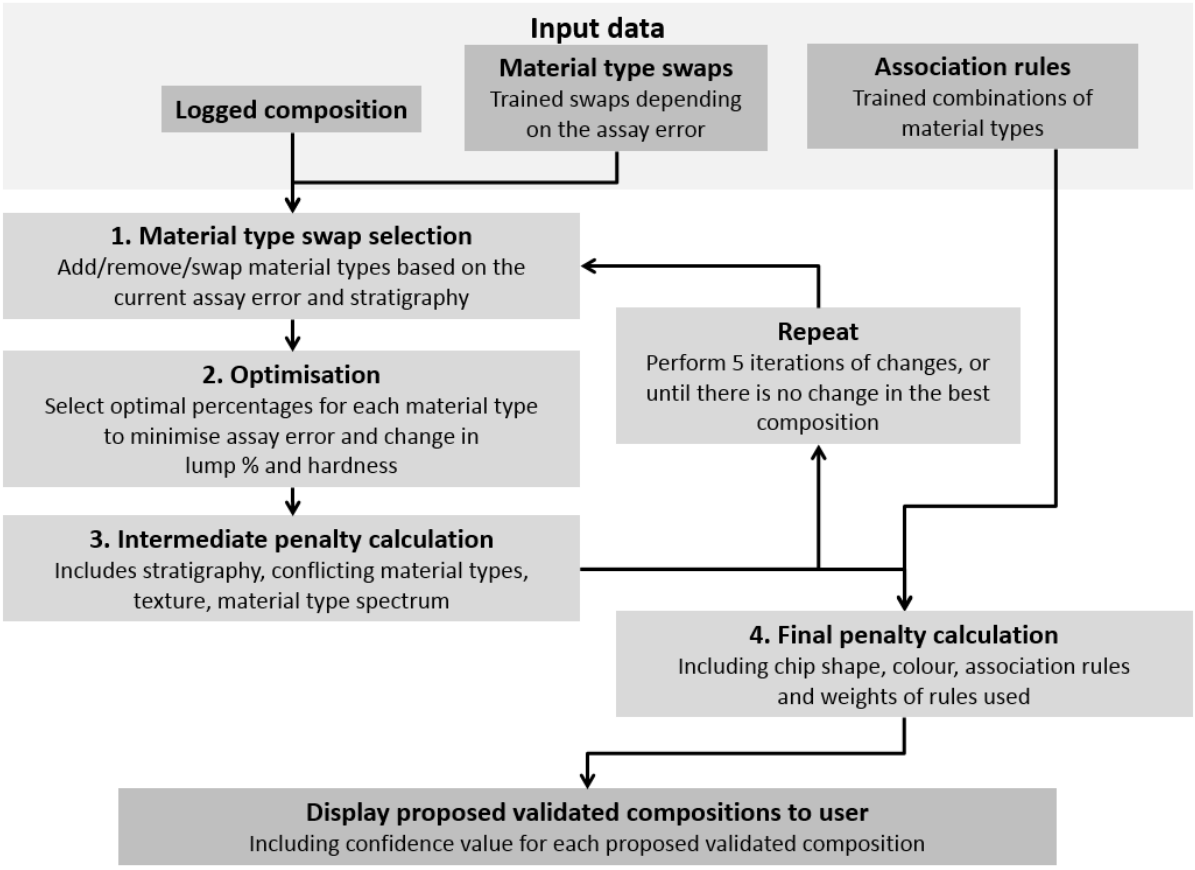

Figure 4: Summary of the AVA algorithm.

Material type swap selection

Material type swaps are selected from the validation rules learned from users during the training phase. Each validation rule was defined with a normalized assay error, a material type with increased percentage, a material type with reduced percentage, stratigraphic class, and weight (i.e. the total amount of material swapped according to that assay error vector during training). The chemical element with the greatest percentage error is determined, which we define as the dominant element. Rules are then selected in three phases.

The first phase selects rules with a dominant element value of -1 or 1, which are the rules that were applied in training to predominantly correct errors in the dominant element. If the rule's dominant element is of opposite sign to the dominant element in the current assay error vector, the rule is inverted by negating the rule's assay error vector, and switching the material types to be added and removed. Then, any rules attempting to remove material types not present in the current intermediate state's composition are discarded. Even though the dominant elements are the same, the other assay error elements may be significantly different, and so we compute the angle between the current assay error vector and each rule's normalized assay error vector; rules with an angle greater than 45 degrees from the current assay error are disregarded. This angle was chosen empirically, as it allows for a variety of rules to be selected while keeping the algorithm's speed acceptable.

The remaining rules provide a list of potential material type swaps to apply. Some material type swaps may be duplicated, as they are represented by different assay error vectors; these duplicates are merged and the weights of the corresponding rules summed. The list of potential swaps are then sorted by the weights of each rule, in order to preferentially apply swaps that have historically been more commonly applied.

In the second phase, the element of the assay error vector with the second greatest magnitude is used instead for filtering, selecting rules, and summing weights of duplicated swaps as above;

finally the third greatest magnitude element of the assay error vector is used similarly in the third phase. Using the three largest elements provides robustness to errors, and allows the algorithm to select rules that are optimal for three dominant elements to provide a better overall solution within a reasonable computational time.

In addition, for some dominant elements, manually crafted rules are added for specific material types related to that element, as these scenarios may have occurred infrequently in the training dataset. For example, if the theoretical alumina value needs to be increased but not the silica value, add the gibbsite and/or aluminous goethite material type. There are 15 rules, covering the trace elements CaO, MgO, Mn, P and S, in each of the three stratigraphic classes.

The material type swaps are applied in parallel, thus the selected intermediate states branch-out to multiple child states, each with a unique set of material types. At this stage, only the set of present material types is altered – the actual percentages of each type are determined in the optimization step. Note that if altering the composition would result in the set of material types matching those of a composition from an earlier state, the state is discarded to avoid revisiting a previously processed state.

Optimization

The percentages for each material type are calculated by minimizing a *cost function* that incorporates three aspects: assay errors, changes in mineral hardness, and changes in lump percentage. We now discuss the cost function components and constraints before describing the optimization method details.

Assay errors: We define assay errors in terms of an assay error tolerance factor, which is the proportion of the assay percentage error relative to a predetermined tolerance value for each element; a tolerance factor of 1 therefore represents the largest allowable absolute error for that element. The tolerances are set independently for each element and may vary from project to project according to requirements, or according to the interval's iron grade, as less accurate validation is required for low-grade (waste) intervals. Typically the tolerances in the assay error for Fe and SiO_2 are 2.5%, for Al_2O_3 2%, and the total LOI tolerance is 1.5%. All solutions having theoretical assay values within the respective tolerance of the laboratory assay value are considered equally valid. Assay error tolerance factors less than 0.5 are rounded to 0.5 to avoid over-optimization, since material type percentages are generally presented to the user as integer values for simplicity.

Mathematically, for assay element *a*, laboratory assay value *L*, theoretical assay value *T*, error tolerance ε, and tolerance factor weighting *f*, the assay error component E_{assay} is given by:

$$E_{assay} = \sum_{a} \frac{\max(|L_a - T_a|, \varepsilon_a/2)}{\varepsilon_a} * f_a$$

where f=2 for Fe, SiO_2 and Al_2O_3 and 1 otherwise, emphasizing the relative significance of errors in these elements, and the max(,) function returns the maximum value of the two arguments.

Changes in mineral hardness: The mineral hardness component aims to preserve the logged composition's distribution of RC chip hardness, divided into three hardness bins comprising hard, medium and friable material types. The intermediate state's composition is partitioned similarly. The differences of corresponding bin values are taken, minus a grace change in hardness of 10% allowing for minor changes in hardness without penalty. A change in hardness Δ_h is computed over *H*ard, *M*edium and *F*riable bin indices *b* within the logged composition B_{logged} and optimized composition $B_{optimized}$:

$$\Delta_h = \sum_{b \in \{H,M,F\}} \max(|B^b_{logged} - B^b_{optimized}| - 0.1, 0),$$

where the max function prevents negative values after subtracting the grace change in hardness. The hardness error component $E_{hardness}$ is given using a Gaussian function:

$$E_{hardness} = \exp(-\frac{\Delta_h^2}{0.3 * 0.25^2}),$$

where the constant term 0.3 to adjust the weighting was determined empirically, and the standard deviation value of 0.25 was derived from the training data.

Changes in lump percentage: The lump percentage for each material type measures the breakdown into lump (nominally particles >6.3mm or 0.25" in diameter) and fines products. Although the hardness in the logged data is a qualitative material property, the lump percentage gives a quantitative measure. Importantly, the grades of the same material type can vary for the resulting lump and fines product (typically the Fe grade is higher for lump product). Since lump and fines products are marketed separately, these changes are significant. We aim to match the theoretical lump percent for the intermediate state to that of the logged composition. A sigmoid function is used to calculate a lump error component E_{lump} from the change in the lump percentage Δ_l:

$$E_{lump} = 0.5 + \frac{1}{2 + \left(\frac{\Delta_l}{50}\right)^2}$$

The denominator of 50 in the squared term controls the dropoff rate of the error value. The result ranges from 2/3 (when Δ_l is at its maximum value of 100) to a maximum of 1 (when $\Delta_l = 0$).

Optimization algorithm: The cost function is defined using assay errors, E_{assay}, changes in mineral hardness, $E_{hardness}$, and changes in lump percentage, E_{lump} :

$$E_{total} = \frac{E_{assay} * E_{hardness}}{E_{lump}} * (1 + n)$$

where *n* is the number of assay elements with errors greater than that element's tolerance.

The optimization function uses boundary and linear equality constraints and is implemented by the optimization package ALGLIB (http://www.alglib.net, Sergey Bochkanov). The boundary constraints ensure that each material type's percentage lies between 0 and the maximum value that would cause the theoretical value for any element to exceed the laboratory assay value by the error tolerance. Further bounds are applied to specific material types identified as *textural* types such as pisolite, where only a small variation in percentage is allowed, for example, ± 10%, as well as ensuring that the type should not be removed entirely (if less than 10% is logged). Textural types are rarely confused with other types, and so the field geologist's logging should not be significantly modified. Finally, a linear constraint ensures that the material types' percentages sum to 100%.

The optimization process converges to a local minimum of the cost function given the constraints. Due to the wide variations in possible optimization constraints and theoretical assay compositions, we are unable to prove analytically that a global minimum is located, though in practice, we have observed that a wide range of initial starting parameters converge to the same local minimum. Therefore, when applying the validation rules, we do not need to directly swap a given percentage of material type 1 for the same percentage of material type 2; the optimization function calculates the percentages for the new set of material types that best fit the laboratory assays, hardness distribution, and the lump percentage.

Intermediate state penalty calculation

The intermediate state penalty is applied to each intermediate state to penalize geologically unusual combinations of material types. It is a numeric multiplier applied to the state's cost value. Since it is only dependent on the set of material types (not the percentages) it can be computed after the optimization for each composition, rather than inside every calculation of the cost function. Large penalty multipliers (such as 4 or 8) have been used so that an assay match must be significantly better to counteract the geological penalty. Several geological characteristics are considered, and where the same characteristic is violated multiple times, penalties are applied repeatedly for each violation within each intermediate state. Penalties do not accumulate between successive intermediate states.

Stratigraphy: Material type swap rules are applied preferentially from the same stratigraphic class as the interval being validated by applying a penalty to rules trained from other stratigraphies. For training rules from a different stratigraphy, we apply a penalty rather than banning them altogether in order to broaden the set of possible rules, particularly when there are few rules with similar assay errors to the current state. If a rule introduces a material type that is prohibited in a particular stratigraphy, the geological inconsistency will be detected by one of the following penalties. It is important to note that the stratigraphic class may be incorrectly logged, in which case this penalty will

still apply, however applying a penalty is preferable to only selecting rules from within only the selected stratigraphy. Further, in the majority of intervals where the stratigraphy is correctly logged, this penalty results in the selection of more appropriate rules.

Conflicting and prohibited material types: Some material type combinations are geologically forbidden. For example, the MTCS contains three silica material types for different geological scenarios: the quartz and secondary silica types indicate hydration, and are used in detrital strata, and to mark faults, whereas the chert type is only used in unhydrated bedded strata. Although chemically identical for matching assay values and grade estimation, using the wrong type may lead to geological misunderstandings during modeling; applying a penalty prevents these situations. Similarly, kaolinite is logged as the clay type in hydrated and detrital intervals, but as the shale type in un-hydrated intervals. We also apply a penalty for combining end member material types predominantly consisting of one element. For example, using gibbsite (alumina) together with quartz (silica), in place of a kaolinite type which is high in both elements and is more likely geologically.

Texture: Some material types have distinctive textures and their presence is obvious. If one of these types is logged, a penalty is applied if the type is completely removed during validation. A penalty is also applied for adding one of these material types if not originally logged.

Hydration: Some material types, such as vitreous goethite, have characteristics arising from hydration and should only be included if the interval is in a known hydrated zone. Conversely, some material types are less common in the hydrated zone, such as the chert and shale types. We apply penalties for using hydrated types in non-hydrated intervals or vice-versa. Even though LOI is indicative of hydration, some types are a by-product of hydration and will not have any LOI signature, for example precipitated silica. Additionally, while some goethite types have the same LOI signature, vitreous goethite is only found in the hydrated zone.

Hematite-goethite continuity: As shown in **Error! Reference source not found.**, there are material types representing various compositions of hematite and goethite at different levels of hardness: H2H, H2M and H2F all represent predominantly hematitic material that for simplicity is classified respectively as hard, medium and friable. In practice, however, there is a continuous spectrum of hardness, and it is unusual for the H2H and H2F types to be logged together without the H2M code. A penalty is applied when the hardness spectrum continuity is broken. In another aspect, the MTCS also contains predominantly goethitic types of varying hardness (GOV, GOE, GOL) and intermediate hematite-goethite types (HGH, HGM, HGF). As it is similarly unusual for a predominantly goethitic type to be logged alongside a predominantly hematitic type if an intermediate type is not also logged, this discontinuity is also penalized.

These penalties are accumulated and applied to the cost computed previously. The 40 states with the lowest product of the cost function value and intermediate state penalty are then used as the basis for the next iteration, or for selecting the final proposed validations.

Selection of final proposed validations

The final stage of composition selection penalizes unlikely material type compositions by analyzing statistics of material type occurrences and co-occurrences, and the weights of the validation rules applied in each iteration. By applying this penalty as a final step, we analyze the final composition only, whereas analyzing intermediate states may penalize locally suboptimal paths to a satisfactory final composition.

Each interval has up to two colors logged. For each material type in an interval, the number of occurrences of that type having the logged color in the historical training data is retrieved and multiplied by that type's composition percentage in the interval. These products are summed over each logged material type to give the color confidence p_{col}. To avoid small values arising where little training data is available, a minimum value of 0.5 is applied, thus $0.5 \leq c_{col} \leq 1$. Similarly, the proportions of the logged chip shapes (either angular, sub-angular, rounded, sub-rounded, or combinations thereof), and stratigraphic class for each material type are examined. The resulting chip shape confidence c_{chip} satisfies $0.5 \leq c_{chip} \leq 1$, and similarly $0.5 \leq c_{strat} \leq 1$ for the stratigraphy proportion c_{strat}.

Since material type swap rules that were more commonly performed by validators during training are preferred, a rule weight based on the training rules' weights is calculated. In each iteration, an applied rule's weight is normalized by the maximum weight of a rule applied (in any

intermediate state) for that iteration, to avoid a single rule from one iteration influencing the weights of rules in other iterations. The rule weight w is the sum of the normalized rules over all five iterations, and will be a value greater than zero and less than or equal to 5; larger values are preferred.

We wish to respect the geologist's logging by minimizing the number of material types changed, *S*. Note that adding one type is one change, and subtracting one type is also one change; completely swapping one type for another is two changes.

Finally, we consider geologically unusual combinations of material types not seen in the training data. For a novel combination, a score is calculated based on the association rules and confidence values mined by the Apriori algorithm. The score is computed for a set of *N* material types by first enumerating all subsets of *N*-1 material types. For a given subset *S*, if an association rule exists for the subset, the score is the highest confidence value for the individual material types m_1 and m_2, where $m_1 \in S$ and $m_2 \notin S$. If no association rule exists satisfying any subset and constituent material types, a similar process is performed for subsets of size *N*-2, and the score computed using the product of the two confidence values corresponding to the missing material types. The association confidence value, c_{assoc}, is therefore greater than 0 and less than or equal to 1.

The final penalty p_{final} is computed from these components, where low confidence values incur a larger penalty:

$$p_{final} = \frac{1}{c_{col} * c_{chip} * c_{strat} * max(1,S) * w * c_{assoc}}$$

The algorithm ranks the validated compositions on $E_{total} + p_{final}$. This sum is then mapped to an integer confidence value from 1 to 10 in order to scale the penalty for convenient interpretation by the geologist, and the top ten compositions presented to the geologist with the confidence values, as potential validated compositions. The geologist can select a proposed composition or perform manual validation. Upon selecting a proposed composition, the validator can further modify the composition before saving it as the *final validated composition*.

AVA's structure is inspired by the particle filter (Arulampalam et al., 2002), but uses trained rules in place of a randomized resampling step, and each iteration corresponds to change in material type composition, rather than a time step.

Updating training data

We designed the algorithm and training data to allow editing and incremental addition of training data without reprocessing the entire training dataset. This includes expanding the training dataset when gaps are found, such as specific assay error scenarios, or where particular material types are not handled.

The weights of material swap rules can be modified, either directly or through selecting intervals that were auto-validated using AVA. Each interval validated by AVA records the rules applied in each intermediate state. The percentage of material swapped according to a rule at a given state is then added to that rule's existing weight. Since the rule weights are used in calculating the final penalty, this causes those rules to become more accepted by AVA over time.

Specific material type association rules can also be interrogated, added or removed, thus altering the allowed combinations of material types which are used in calculating the final penalty.

Results and Discussion

The algorithm's performance was evaluated in two experiments. We first assessed the accuracy of the proposed validated compositions by analyzing the proposed compositions selected by expert geologists. In the second experiment, AVA was applied in a batch manner to an entire deposit to examine the distributions of specific material types.

In the first experiment, a select group of geologists validated 1,996 intervals from deposits across the Hamersley province, covering variations in geology and material type geochemistry. Importantly, these evaluation intervals were different to the intervals used in the training process. In 1,483 (74.3%) intervals, the geologist selected an auto-validated composition and accepted it as the final validated composition without further change. Importantly, of these selected compositions, the

composition with the highest confidence was selected 833 times (56.2% of intervals) while the mean ranking of the selected composition was 2.1, demonstrating that validation can be expedited by presenting fewer options to the user.

Of the remaining 513 intervals that were not selected without change, for 187 intervals, the geologist retained the same set of material types selected by AVA and modified their percentages only, in order to change the hardness or theoretical lump percentage. Therefore, the geologist was satisfied with the set of material types selected by AVA in 1,670 of the 1,996 intervals (83.7%). In a further 49 of the remaining 326 intervals, the geologist modified the selected auto-validated composition by substituting material types within the same family. For example, substituting hard hematite-goethite (HGH) for the medium-hardness hematite-goethite (HGM), to preserve the logged hardness while accepting the composition's mineralogy. These results are summarized in **Error! Reference source not found.**.

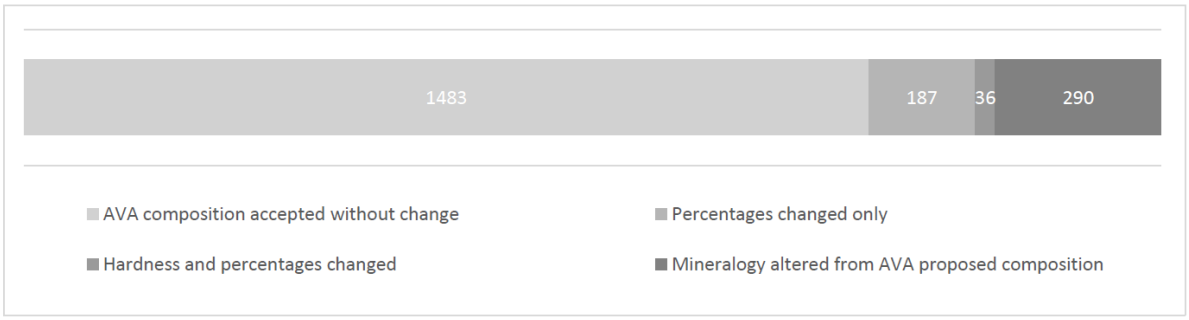

Figure 5: A summary of the final compositions accepted by the geologist after processing intervals with AVA.

These results demonstrate that for the majority of intervals, AVA selects a set of material types geologically acceptable to the geologist. This reduces the time to process each interval significantly, and for the intervals where the geologist is not satisfied with the proposed auto-validated compositions, manual validation can still be performed with only a small time penalty for comparing the AVA results.

In the second experiment, AVA was used to validate an entire deposit containing over 14,600 intervals. All intervals in this deposit were routinely manually validated previously, against which AVA's results were compared; the original logged composition for each interval was provided as input for AVA. Importantly, the manual validations for these intervals were not used in providing training data for AVA. We evaluated the top-ranked auto-validated composition (i.e. highest confidence value) for each interval. We measured three aspects: errors between the laboratory and theoretical assays for the logged composition, manually validated composition and the top-ranked auto-validated composition; a comparison of the hardness distribution of the logged, manually validated and top-ranked auto-validated compositions; and the percentages of ochreous goethite and kaolinite (shale/clay material types), which are commonly confused. For these comparisons, the results are broken down by stratigraphic class: detrital intervals, mineralized bedded intervals, and shale intervals. Note that local variations exist within each class; there may exist narrow shale bands within the bedded mineralized class.

We first examine the mean error tolerance factors for each of the logged, manually validated and auto-validated compositions for the most significant elements for mineralized (Fe > 55%) intervals in Figure 6A, and all intervals in Figure 6B. The mean error tolerance factors, and the 25th and 75th percentile values are shown. We used these percentiles rather than a standard deviation, since the standard deviation is significantly increased by a small number of unmineralized intervals with large error tolerance factor values. In practice, the AVA informs the user that the proposed solution is of low confidence for these intervals. The presence of these outliers is still visible in some cases, such as where the mean AVA error tolerance for the Total LOI for all intervals is roughly equal to the 75^{th} percentile.

The mean error tolerance factors of the manually and auto-validated compositions are significantly less than for the logged composition, highlighting the importance and need for validation. In the mineralized intervals (Fig. 6A), the mean error tolerance factors and interquartile ranges for the auto-validated compositions are similar to those of the manually-validated compositions, but where waste intervals are included (Fig. 6B), the auto-validated compositions generally have lower errors. This is partly due to greater variability in the geology in waste intervals, which makes validation more complex; accurate validation is less important in these intervals, as they do not form crusher feed.

Of interest is the magnitude of the error tolerance factors for the mineralized intervals. Significantly, even though the cost function applies a lower bound of 0.5 to each element's error tolerance factor, yet for these important elements the mean error tolerance is consistently less than that value. This indicates that the auto-validated composition accurately matches the assays, while retaining the logged hardness and lump percentage.

(A)

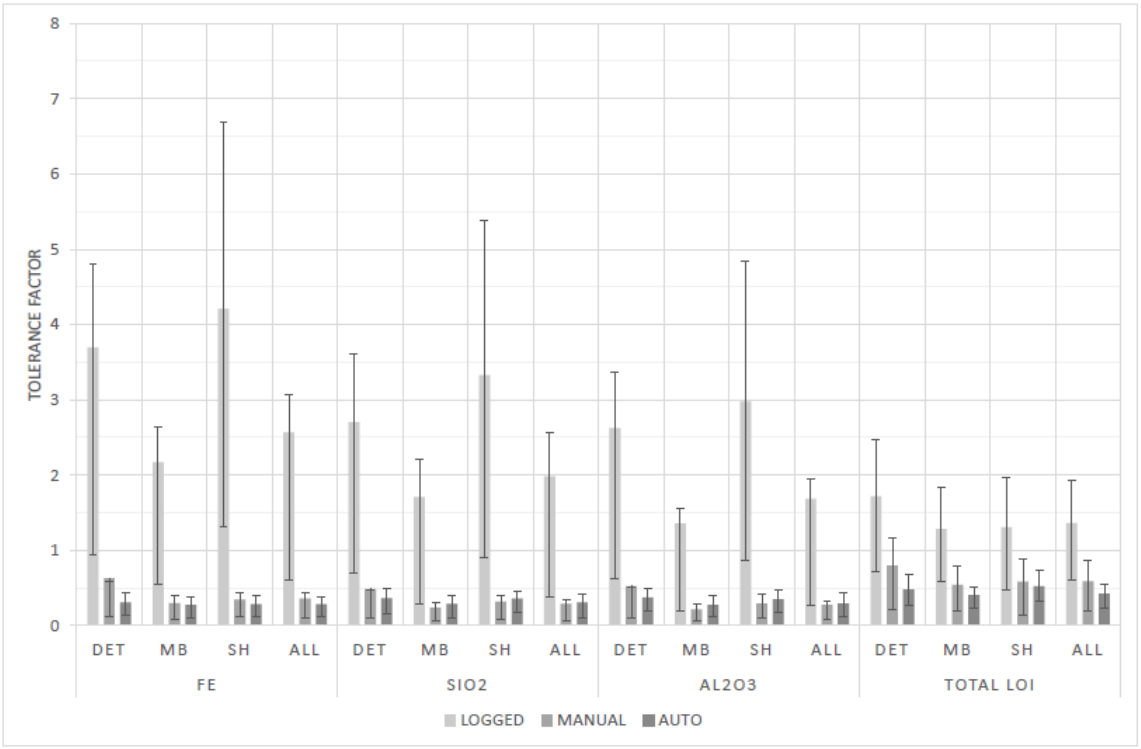

(B)

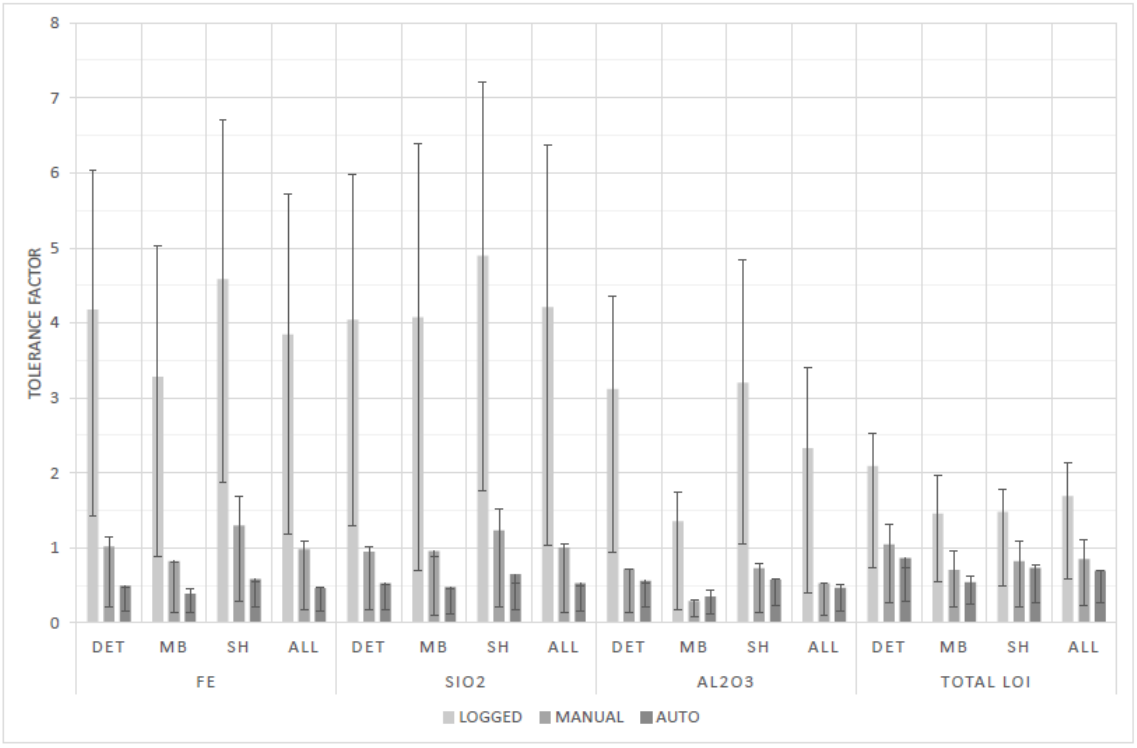

Figure 6: (A) Mean error tolerance factors for selected elements for mineralized intervals (Fe > 55%). (B) Error tolerance factor for selected elements for all intervals. Error bars display values for the 25th and 75th percentiles. The intervals are divided by stratigraphy: detritals (DET), mineralized bedded (MB), shales (SH), and all intervals.

In Figure 7 we evaluate the mean change in compositions' hardness bin distributions (hard, medium and friable) for manual and automated validation. These percentages record double the actual material moved between bins, since moving 10% of material from hard to medium is a 10% reduction in hard material plus a 10% increase in medium material, counted as 20%. Similar to the error tolerance factor, for auto-validated compositions, the change in hardness is comparable to manual validated compositions for mineralized intervals, but over all intervals, the AVA's change in hardness is significantly lower than for manual validations.

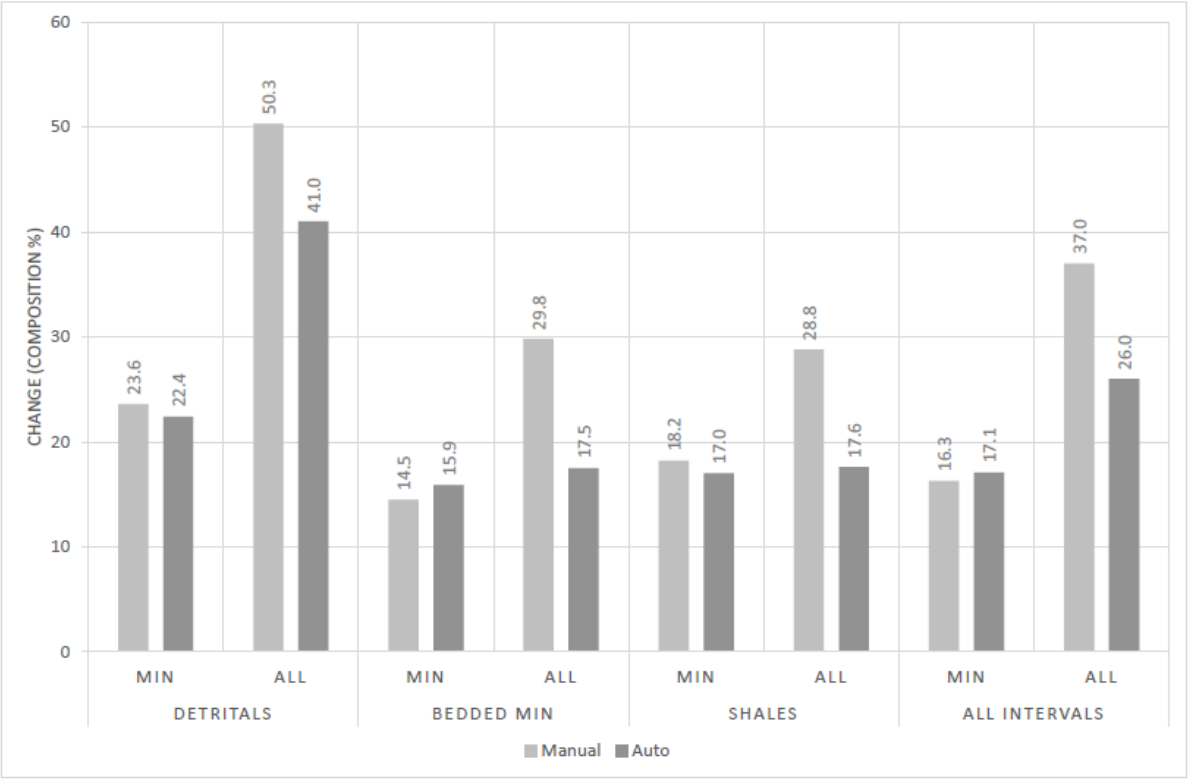

Figure 7: The percentage changes in hardness for mineralized (Fe > 55%) intervals only (MIN), and all intervals (ALL).

Finally, the proportions of ochreous goethite and kaolinite material are examined. These two material type classes are commonly confused during logging, and accurately identifying these types in validation is essential to avoid grade errors and handling problems. Figure 8A shows that the mean logged percentage of ochreous goethite types is consistently lower than the mean validated percentages. Conversely, Figure 8B shows that manual validation consistently produces compositions with lower kaolinite content than was originally logged, illustrating a bias towards over-logging kaolinite types of over 20% on average in mineralized shale-class intervals. This, unsurprisingly, is most evident in shale class intervals.

The net changes in kaolinite and ochreous goethite types during validation are summarized in Figure 9. Comparing the logged percentages of each, we see that the mean decrease in kaolinite percentage typically is greater than the increase in ochreous goethites for both manual and auto-validated compositions. This is because it is not a direct 1:1 swap: some kaolinite may instead be swapped for the HGF material type, another common material type swap highlighted in Figure 3A.

(A)

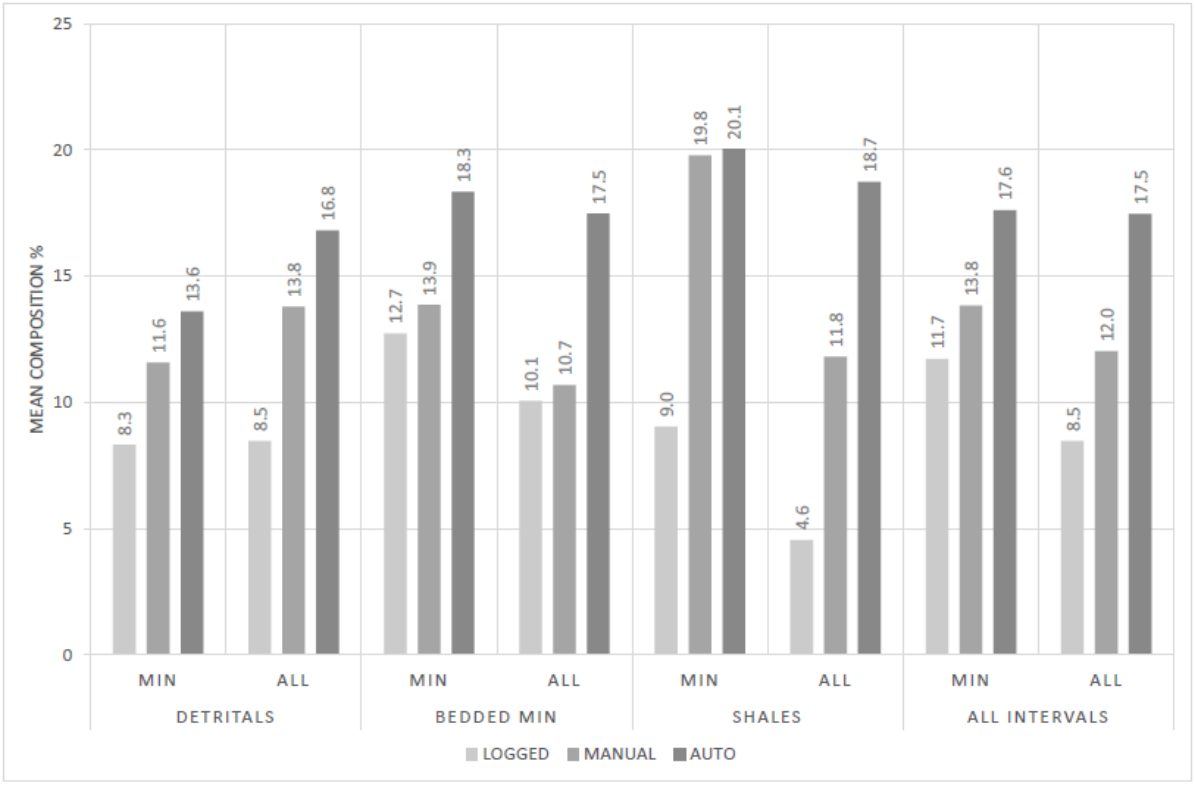

(B)

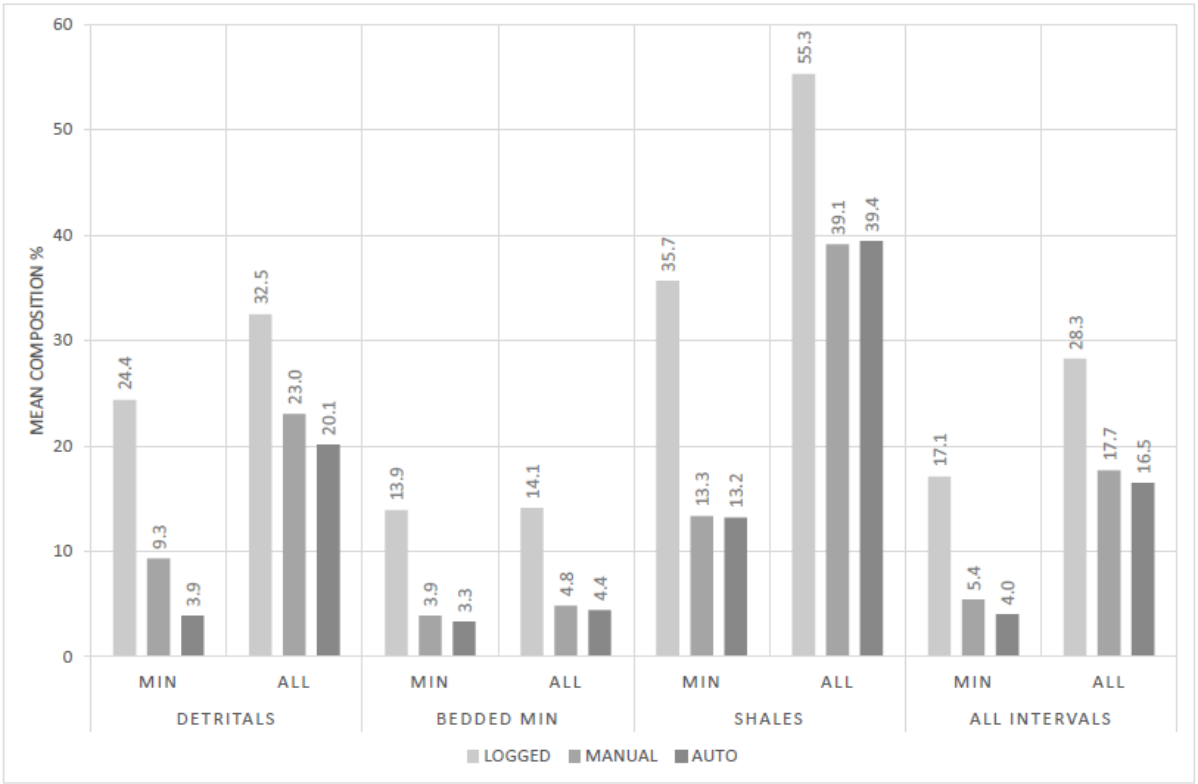

Figure 8: (A) Ochreous goethite compositions for mineralized (MIN) and all intervals, broken down by stratigraphy. (B) Kaolinite compositions for mineralized (MIN) and all intervals, broken down by stratigraphy.

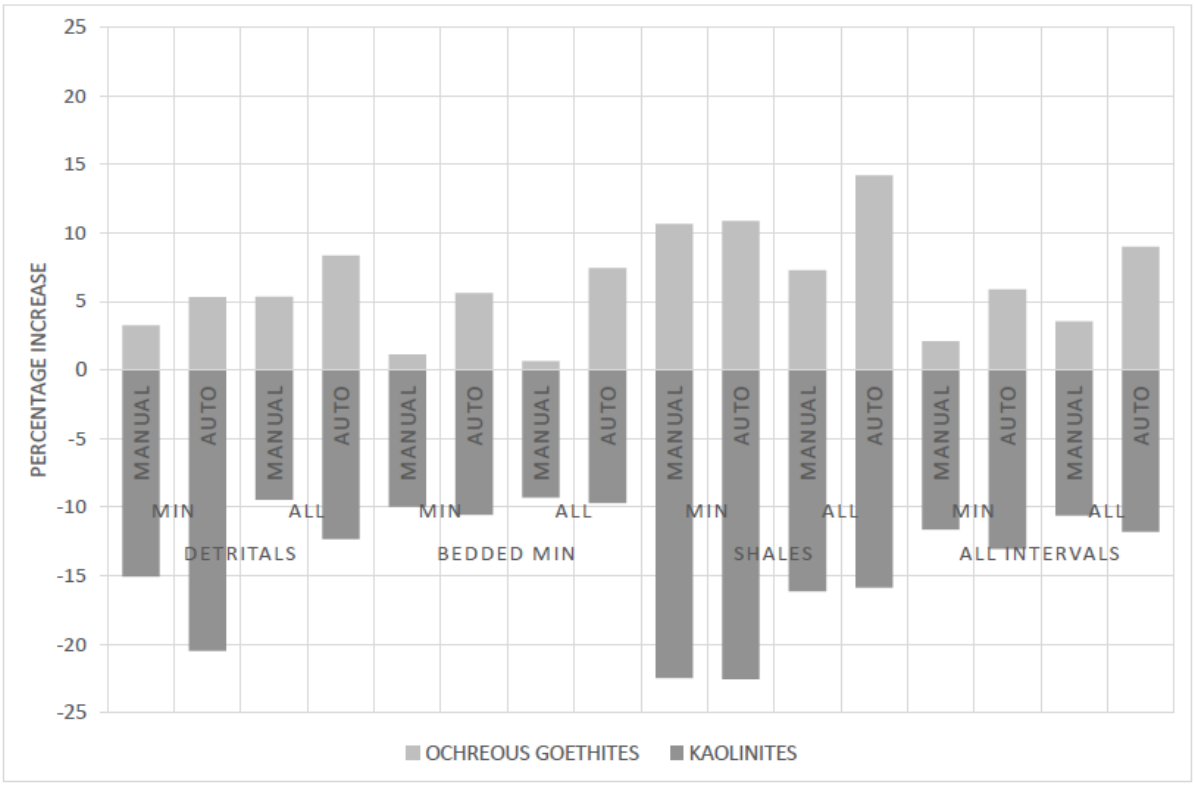

Figure 9: A summary of the mean changes in composition in manual and auto-validated ochreous goethites and kaolinite types, compared to the logged composition.

Conclusions

The AVA algorithm was developed to improve the integrity of drillhole logging data. It validates material type compositions for an interval to match the laboratory assay values, using validation rules learned from geologists in a training phase, and performs geologically informed exchanges of material types. The validated compositions contain geologically valid combinations of material types satisfying geological, geochemical and physical constraints.

The algorithm's accuracy is comparable to manual validation for mineralized intervals, and provides better matches to the laboratory assays overall when low-grade intervals are considered. Additionally, using AVA transforms the laborious validation process to a decision making step, while the geologist retains control of the final validated composition. AVA enables geologists to process their field logging rapidly and consistently, leading to savings in labor and improved orebody modeling.

Acknowledgements

We thank Rio Tinto Iron Ore for funding this research and in particular the geologists that spent countless hours validating samples to satiate AVA's appetite for information.

References

Agrawal, R. and Srikant, R., 1994, Fast Algorithms for Mining Association Rules: Proceedings of the 20th Very Large Data Base Conference, Santiago, Chile, p. 487–499.

Arulampalam, M.S., Maskell, S., Gordon, N. J. & Clapp, T., 2002, A Tutorial on Particle Filters for Online Nonlinear/Non-Gaussian Bayesian Tracking: IEEE Transactions on Signal Processing, 50(2), 2002, p. 174–188.

Box, J., Phillips, J., and Clout, J., 2002. Use of geological material types for predicting iron ore product characteristics: FUWA - Ward Iron and Steel Making Workshop, April 4th – 5th 2002.

Morris R.C. 1994, Detrital Iron Deposits of the Hamersley Province: CSIRO Division of Exploration and Mining GDSR 2536, 233p.

Paine, M.D., Boyle, C., Lewan, A., Phuak, E., Mackenzie, P., Ryan, E., 2016, Geometallurgy at RTIO – a new angle on an old concept: Third AusIMM International Geometallurgy Conference, p. 55–61.

Sommerville, B., Boyle, C., Brajkovich, N., Savory, P. and A.-A. Latscha, A.-A., 2014, Mineral resource estimation of the Brockman 4 iron ore deposit in the Pilbara region: Special Issue on Mineral Resource Estimation, Applied Earth Science, p. 135–145.

Trendall, A. F. and Blockley, J. G., 1970, The iron formations of the Precambrian Hamersley Group, Western Australia, with special reference to the associated crocidolite: Bulletin 119, Geological Survey of Western Australia, 365p.